Research Article

Journal of Environmental Nanotechnology

Influence of TiO_2 Nanoparticles on Engine Parameters at Varied Compression Ratio of CI Engine Fuelled with Biodiesel

V. Hariram[1*], V. Ramanathan[2], A. John Presin Kumar[1], J. Allen Jeffrey[3], R. Christu Paul[2], A. Manigandan[3], R. Selvakumar[2] and D. Balaji[1]

[1]Department of Mechanical Engineering, Hindustan Institute of Technology and Science, Padur, Chennai, TN, India
[2]Department of Automobile Engineering, Hindustan Institute of Technology and Science, Padur, Chennai, TN, India
[3]Department of Mechanical Engineering, Loyola Institute of Technology, Chennai, TN, India
Received: 22.04.2025 Accepted: 21.05.2025 Published: 30.06.2025
*connect2hariram@gmail.com

ABSTRACT

Despite benefits like renewability, biodegradability, non-toxic nature, and reduced pollution emissions, widespread use of biodiesel as a diesel replacement faces obstacles such as lower-energy output, high viscosity, suboptimal atomization, increased density and elevated NO_x emissions. This study emphasizes on comparing and assessing the emission, combustion and performance of a fuel blend made of 20% *Chlorella* biodiesel and 80% diesel from *Chlorella* bio-oil, enhanced with titanium oxide nanoparticles. D100, D80CvBD20, D80CvBD20$TiO_2$50, D80CvBD20$TiO_2$100, and D80CvBD20$TiO_2$150 fuel blends are among those examined. Experiments were conducted to assess the emissions, combustion and performance phenomenon at compression ratios of 17, 17.5 and 18. The D80CvBD20$TiO_2$100 blend demonstrated superior combustion characteristics by achieving the highest peak cylinder pressure (63.45 bar at 18 CR) and heat-release values. The emission analysis revealed that infusing TiO_2 nanoparticles led to a notable reduction in unburnt hydrocarbons by as much as 13% at higher compression ratios. The nano-fuel blends also exhibited higher NO_x with notable decrease in CO emissions, attributed to enhanced oxygen content and elevated combustion temperatures. The blend D80CvBD20$TiO_2$100 proved to be the most effective and eco-friendly choice due to its prominent reduction in fuel usage and emissions, with the exception of CO_2 and NO_x.

Keyword: Biodiesel; Combustion; *Chlorella vulgaris*; Compression ratio; Titanium oxide.

1. INTRODUCTION

The need to find sustainable energy alternatives has increased due to the impending threat of depletion of fossil fuel supplies and climate change. Algae biodiesel has become a viable option because of its high lipid output and little effect on land use. But some intrinsic drawbacks such as viscosity and oxidative stability prevent it from being widely used. Because of their efficient thermal and catalytic characteristics, nanoparticles provide a viable remedy. Biodiesel, an eco-friendly and renewable fuel extracted from animal or vegetable sources, has aroused as a favourable substitute to fossil diesel due to its potential to significantly decline harmful emissions and decrease dependence on fossil fuels. Algal biodiesel-nanoparticle blends are found to improve engine performance, fuel quality and sustainability (Vellaiyan *et al*. 2020).

Although biodiesel presents a viable alternative to traditional diesel, it is crucial to recognize its health and environmental limitations. Like traditional compression ignition (CI) engines, biodiesel engines release harmful pollutants, including carbon monoxide, nitrogen oxides, unburnt hydrocarbons and particulate matter. Burning biodiesel generates toxins that are linked to many environmental and health issues, even though it comes from renewable sources. These pollutants endanger public health and add to air pollution, which includes smog formation. Moreover, even though it is advantageous in some ways, biodiesels having lower sulphur content have been connected to higher particulate matter emissions. This problem emphasizes how important it is to have efficient emission control plans in order to lessen the negative effects of using biodiesel (Dey *et al.* 2021).

As a substitute to conventional fuels, biodiesel offers promise in reducing the environmental impact of diesel fuel. Nonetheless, a thorough evaluation of its effects necessitates a complete viewpoint of both the advantages and disadvantages related to its emissions. To understand the potential of biodiesel engine emissions as a viable fuel substitute, a comprehensive analysis of the entire conservational impact of these emissions is necessary (John *et al*. 2018). Due to their unique physico-chemical properties, nanoparticles offer a favourable approach to enhancing combustion efficacy and reducing

harmful emissions. Their tiny size and high surface area boost catalytic activity in the exhaust system, facilitating the breakdown of pollutants and improving overall emission control.

Studies have demonstrated that incorporating nanoparticles into biodiesel significantly affects various fuel properties and engine performance parameters. Additionally, the addition of nanoparticles influences the emission of smoke, hydrocarbons, nitrogen oxide and carbon monoxide (Karthikeyan *et al.* 2014). For maximum performance and lowest emissions, compression ignition engines in diesel cars and industrial machinery need effective combustion processes. One interesting method for improving both of these important factors is to incorporate nanoparticles into the biodiesel used in CI engines. Adding nanoparticles to biodiesel can increase the engine's capacity to produce more power. By encouraging full combustion, nanoparticles boost combustion efficiency and catalytic characteristics, which raise engine output. Better fuel economy may arise from the usage of nanoparticles, which increase combustion efficiency. With reduced fuel usage and increased mileage, CI engines operating on nanoparticles-enriched biodiesel blends can save money and emit fewer greenhouse gases.

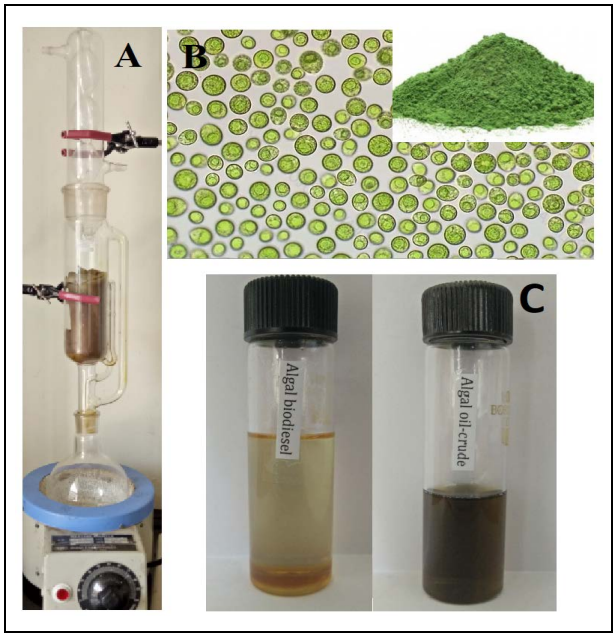


Fig. 1: Biodiesel from *Chlorella vulgaris* microalgae – (A) Microscopic view, (B) Soxhlet bio-oil extraction and (C) Extracted bio-oil and biodiesel

In CI engines, nanoparticles having enhanced catalytic properties have the potential to improve combustion efficiently. Their presence has the potential to reduce ignition delay that occurs between start of combustion and fuel injection. Reduced engine noise and emissions of unburnt hydrocarbons result from rapid ignition, which encourages faster and regulated combustion. Additionally, nanoparticles can enhance combustion stability by promoting more uniform fuel and air mixing, which improves ignition conditions. This reduces the possibility of incomplete combustion and engine knock, which leads to smoother engine operation and lower emissions. Researchers used various biodiesel mixes containing various nanoparticles to study CI engines. A notable improvement in the combustion and performance of CI engines has been observed when operated with numerous bio-diesel blended fuels (Mathimani *et al*. 2015).

Numerous studies have concentrated on the influence of incorporating a diversified nanoparticles into various bio-diesel combinations on the performance of CI engines. The addition of nanoparticles enhances both engine emission phenomenon and combustion characteristics. Based on these observations, this research involves adding nanoparticles to algae biodiesel and examining the resulting emission, performance and combustion, characteristics.

2. MATERIALS AND METHODS

This section details the facts on cultivating *chlorella vulgaris*, collecting its biomass and converting into oil, and biodiesel.

2.1 Cultivation of *Chlorella vulgaris*

Chlorella vulgaris demonstrates the ability to thrive under optimal environmental conditions, with growth parameters such as light intensity, temperature, carbon dioxide and pH. Literature reports suggest that *Chlorella* species produce a higher lipid content compared to the lipid mixture obtained from photoautotrophic and heterotrophic cultures. Optimal growth for *Chlorella vulgaris* is typically observed between 35°C and 25°C. The introduction of carbon dioxide supports chlorophyll synthesis, contributing to both the growth rate and biomass yield. In Bold's Basal medium, nitrogen and phosphorus provided as ammonium nitrate and potassium phosphate, respectively serve as key nutrients, catalysing cellular proliferation and enhancing algal growth. Biomass yields under these conditions range from 0.5 to 2 g/L per day.

2.2 *Chlorella vulgaris* - Biomass Collection and Oil Extraction

To harvest the algal biomass, centrifugation was employed, as this method efficiently utilizes centrifugal force to separate cells grown in the aqueous medium. Following centrifugation, the biomass was filtered through a porous medium to remove the remaining liquid. Additionally, flocculation was implemented to aggregate larger biomass particles, facilitating easier recovery. Once collected, the biomass was dried for subsequent oil extraction.

Fig. 1 shows the procedural method for algal oil extraction from the biomass employing Soxhlet apparatus. The dried algal biomass was placed inside a filter paper thimble, which was subsequently inserted into a glass extraction chamber fitted with an inlet and siphon tube. The assembly was then positioned on a round-bottom flask containing the solvent, which was heated to initiate the process. As the solvent vaporized, it ascended through the inlet tube and condensed upon reaching the condenser. The condensed solvent interacted with the dried biomass, dissolving the oils present. The solution continuously was recycled for 5 hours, and the oil was separated from the solvent through distillation. The microalgal oil was subsequently purified using a rotary evaporator, following the protocol described by Manikandan *et al.* (2020).

2.3 Transesterification

Biodiesel from *Chlorella vulgaris* microalgae was synthesized *via* a single-stage esterification process, utilizing methanol as a solvent and KOH as a catalyst. The chemical reaction led to the breakdown of crude algal bio-oil into biodiesel and glycerol as a by-product. The microalga extract (1000 mL) was placed in a container. Potassium hydroxide was gradually mixed with the methanol, and stirred until completely dissolved. The algal extract was then heated and stirred mechanically within the container. Once the temperature reached 60 ℃, the potassium methoxide solution was introduced while maintaining gentle stirring to ensure complete dissolution. Stirring speed was kept low during this phase to avoid vigorous agitation. Following dissolution, the container was sealed, and stirring was intensified to approximately 720 rpm, with the temperature maintained at 60 ℃ throughout to prevent methanol evaporation (Mehregan *et al.* 2020). After two hours, the mixture was relocated to a separate glass container and allowed to stand for 24 hours, during which biodiesel and glycerol separated. The biodiesel, which floated to the top, was carefully collected after removing the glycerol. The biodiesel was then washed repeatedly to eliminate residual glycerol, and heated at 110 ℃ to evaporate any remaining water, resulting in purified microalgal biodiesel.

3. EXPERIMENTAL SETUP

Table 1 lists the factors of the compression ignition engine employed in the study and also contains the specification of emission analyser, dynamometer, tachometer, smoke analyser, and smoke meter. Fig. 2 displays the engine test bed that is used to assess fuel economy as well as the testing apparatus. The engine's performance characteristics, such as specific fuel consumption, total fuel consumption, brake thermal efficiency, and brake power, were assessed using an eddy current dynamometer and engine software. To conduct experiments with a biodiesel blend, a setup comprising a compression ignition engine, dynamometer, and smoke analyser was used. Kirloskar TV1 model, encompassing 4-stroke, water-cooled, displacement of 661 cc, with a standard compression ratio of 17.5 and stroke/bore length of 110 mm/87.5 mm was employed in this study. An eddy current dynamometer is suitable for evaluating the performance of internal combustion engines, small and medium motors, automotive transmission parts, gas turbines, water turbines, engineering machinery, and oil drilling equipment. By applying a load to the engine's output shaft and observing the resulting outputs, this experiment aims to assess the performance of the engine.

3.1 Error Analysis

The experiments were conducted with the purpose of evaluating uncertainties and errors resulting from human error, environmental conditions, instrument calibration, and reading inaccuracies. To ensure precision, each data point was measured a minimum of five times, and the standard deviation of each measurement was expressed as a percentage and averaged (Mirbagheri *et al.* 2020). Table 2 lists the percentage uncertainties of this study. The total uncertainty was computed using the root mean square method, and the result was 1.72%.

Table 1. Error analysis

Parameters	Uncertainty (%)
Load	0.25
Brake thermal efficiency	1.3
Brake specific fuel consumption	0.9
Engine speed	0.05
Fuel flow rate	0.4
Pressure Transducer	0.20
Crank angle encoder	0.20
Intake air flow	0.12
Time	0.5
NO_x	0.33
UBHC	0.5
CO	0.35
Smoke opacity	0.34

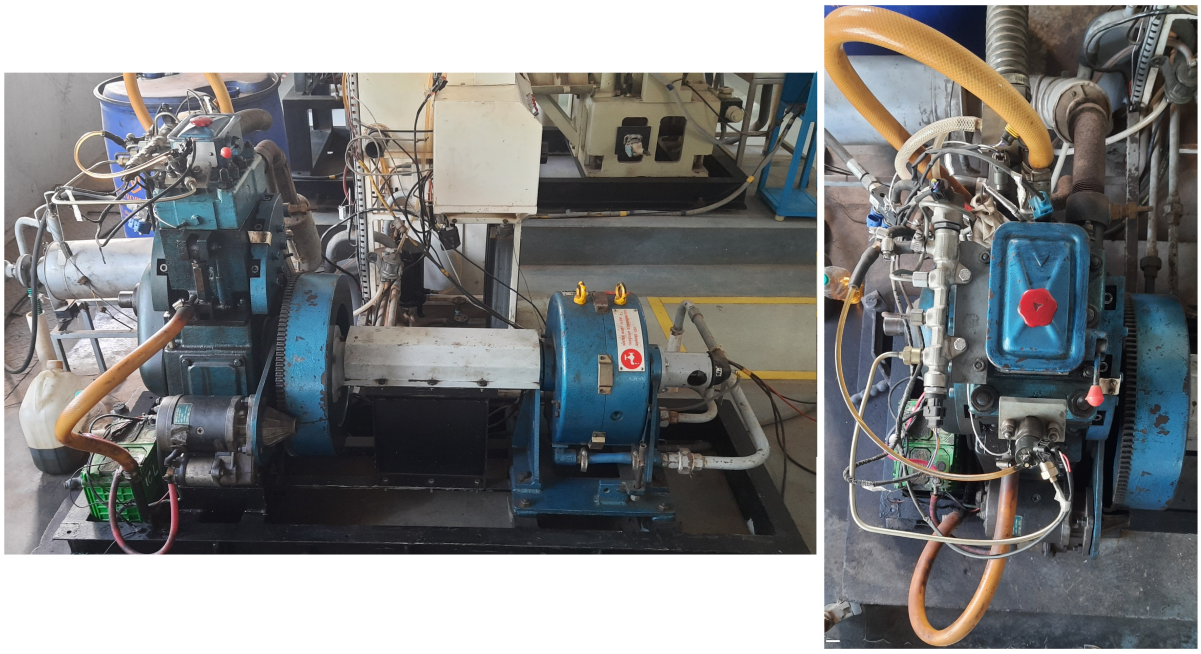


Fig. 2: Engine test rig

Table 2. Specification of test engine and emission analyzer

Make		**Kirloskar TV1**
Bore		110 mm
Stroke		87.5 mm
Rated Power		5.2 kW
Compression ratio / Engine capacity		17.5 / 661 cc
Load sensor		Load cell, type strain gauge, range 0-50 Kg
Rated speed		1500 rpm
Dynamometer		Type eddy current, water cooled
Piezo sensor		Range 5000 PSI, with low noise cable
Instrument	**Measuring parameter**	**Range**
Tachometer	Speed	450–6500 rpm
Smoke meter (AVL)	Smoke opacity	0–100 %
AVL	NO_x	0–6000 ppm
	CO_2	0–22 % vol
	HC	0–3000 ppm
	CO	0–16 % vol

Table 3. Test fuel properties

Properties	**Unit**	**Diesel**	***Chlorella vulgaris* Biodiesel**	**ASTM standard**
Density	Kg/m^3	838	864	ASTM D240
Cloud Point	°C	-16 to 5	7	ASTM D2500
Calorific value	MJ/kg	43.8	41.0	ASTM D240
Pour point	°C	-34 to -16	-7	ASTM D2500
Viscosity (at 4°C)	mm^2/s	1.9-4.2	5.3	ASTM D445
Acid value	Mg KOH/g	0.5	0.375	-
Flash Point	°C	74	115	ASTM D93
Solidification Point	°C	-50 to 10	-12	-
H/C ratio	-	1.83	1.82	-

3.2 Nano-fluid Preparation

TiO_2 nano-fluid biodiesel is a fuel infused with titanium dioxide nanoparticles to enhance its combustion properties and boost overall efficiency. The TiO_2 nanoparticles are dispersed using ultra-sonication in a base fluid which is used to prepare TiO_2 nano-fluid. This biodiesel is left to settle for a while after homogenization to check for stability and make sure that there isn't any noticeable sedimentation of nanoparticles. Diesel and *Chlorella* biodiesel served as the base fuels for this investigation. TiO_2 nanoparticles with an average particle size of 30-50 nm and a purity of 99.9% was employed to augment the properties of test fuel. A B20 mixture (20% biodiesel and 80% diesel) was produced by blending the diesel fuel with *Chlorella* biodiesel. Three different quantities of TiO_2 nanoparticles were added to the mixture: 50, 100, and 150 ppm. An ultrasonicator running at 40 kHz for 45 minutes was used to distribute the TiO_2 nanoparticles in the B20 biodiesel/diesel mixture in order to guarantee a homogeneous blend (Janakiraman *et al.* 2020; Gowtham *et al.* 2020).

3.3 Fuel Properties

The properties of the fuels used in the diesel engine were examined to verify their compliance with standard operating values, and the results are detailed in Table 3.

4. RESULTS AND DISCUSSION

4.1 Performance Analysis

This section will infer the details on performance characteristics of the test fuel blends in terms of brake specific fuel consumption and brake thermal efficiency.

4.1.1 Brake Specific Fuel Consumption (BSFC)

It is a measure of energy expenditure relative to output power, indicating the engine's fuel efficiency. Fig. 3 (A, B, C) illustrates the changes in BSFC with respect to brake mean effective pressure (BMEP) for various fuel blends: diesel (D100), D80CvBD20, D80CvBD20$TiO_2$50, D80CvBD20$TiO_2$100, and D80CvBD20$TiO_2$150.

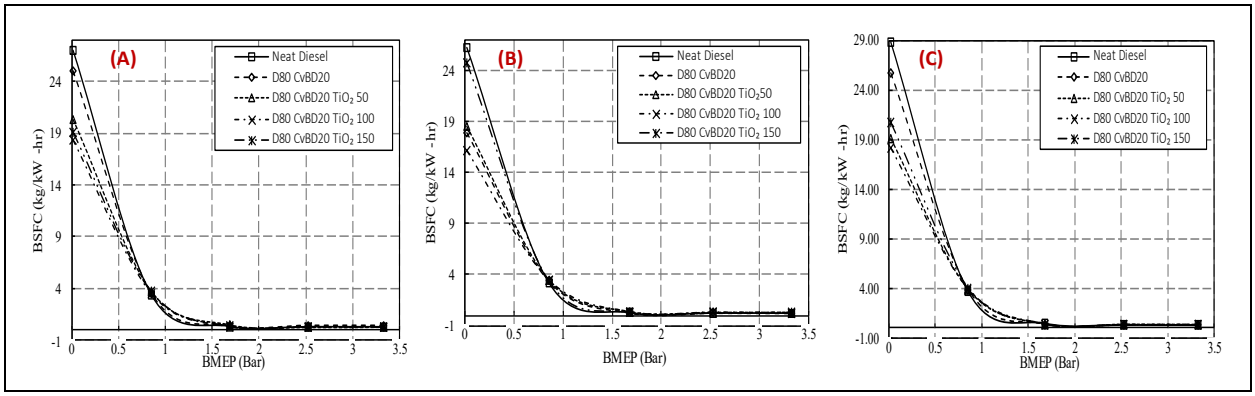


Fig. 3: Variation in BSFC at (A) 17, (B) 17.5 and (C) 18 CR

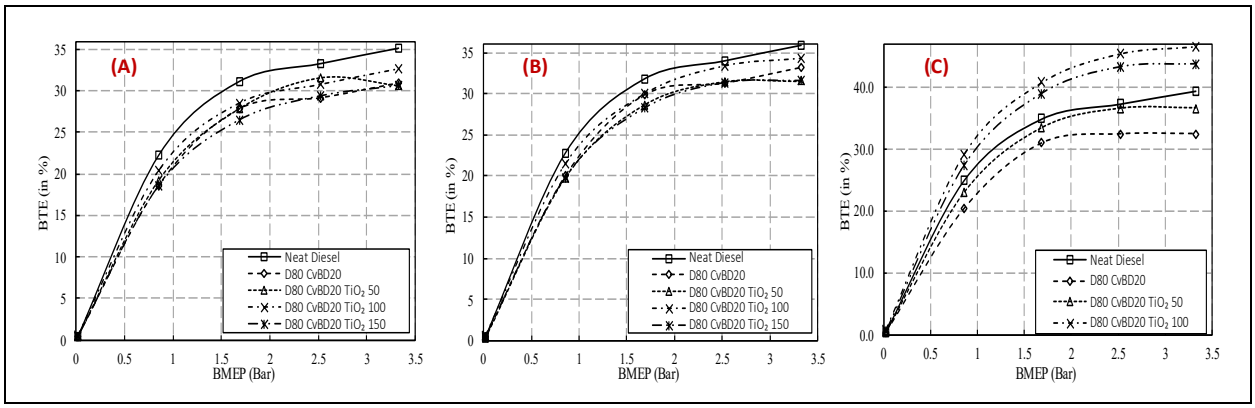


Fig. 4: Variation in BTE at (A) 17, (B) 17.5 and (C) 18 CR

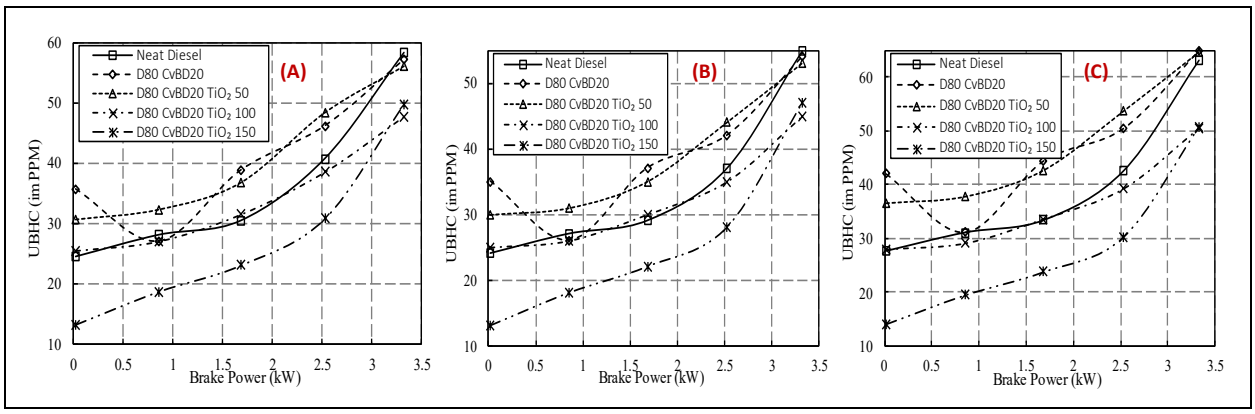


Fig. 5: Variation in UBHC emission at (A) 17, (B) 17.5 and (C) 18 CR

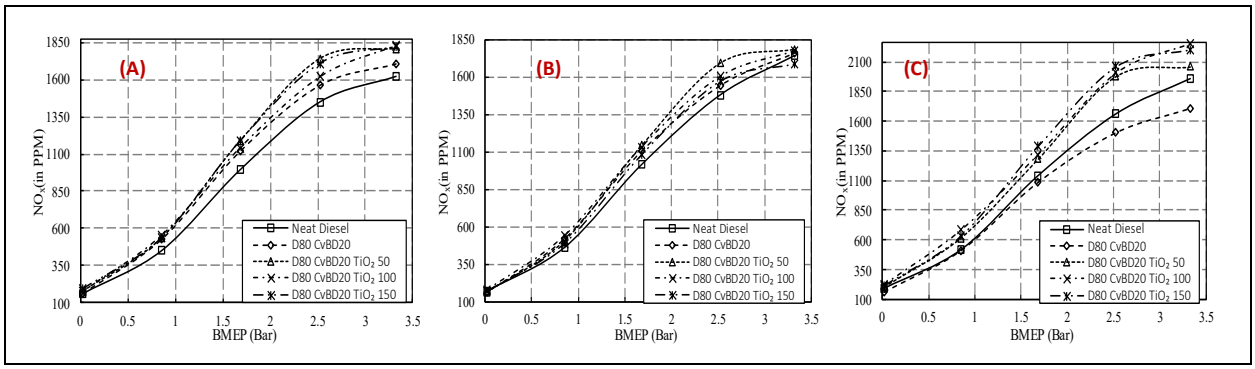


Fig. 6: Variation in NO_x emission at (A) 17, (B) 17.5 and (C) 18 CR

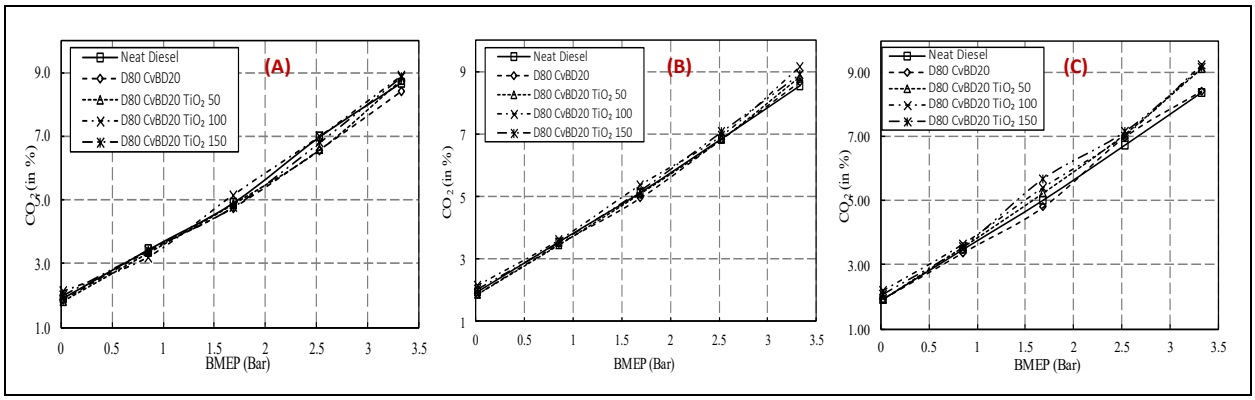


Fig. 7: Variation in CO_2 emission at (A) 17, (B) 17.5 and (C) 18 CR

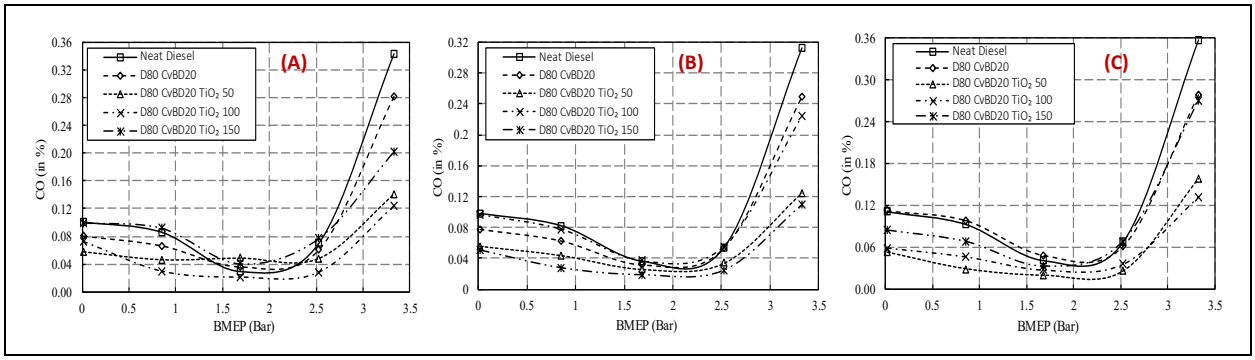


Fig. 8: Variation in CO emission at (A) 17, (B) 17.5 and (C) 18 CR

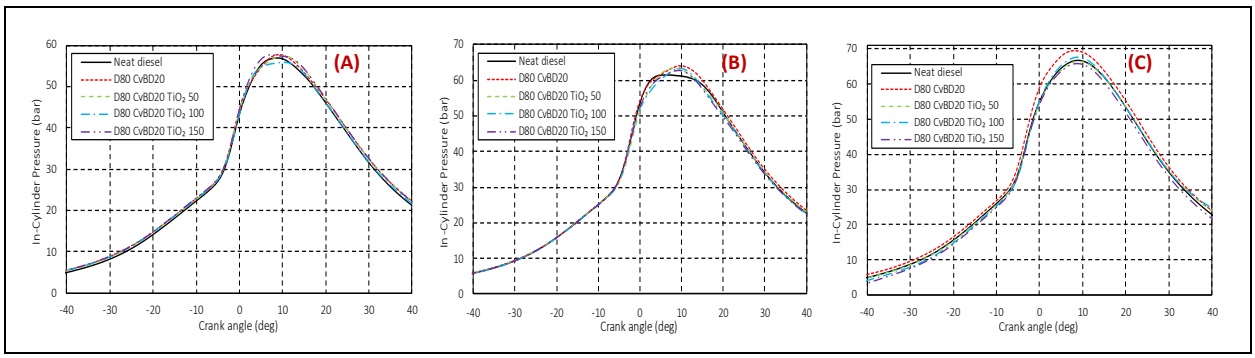


Fig. 9: Variation in in-cylinder pressure at (A) 17, (B) 17.5 and (C) 18 CR

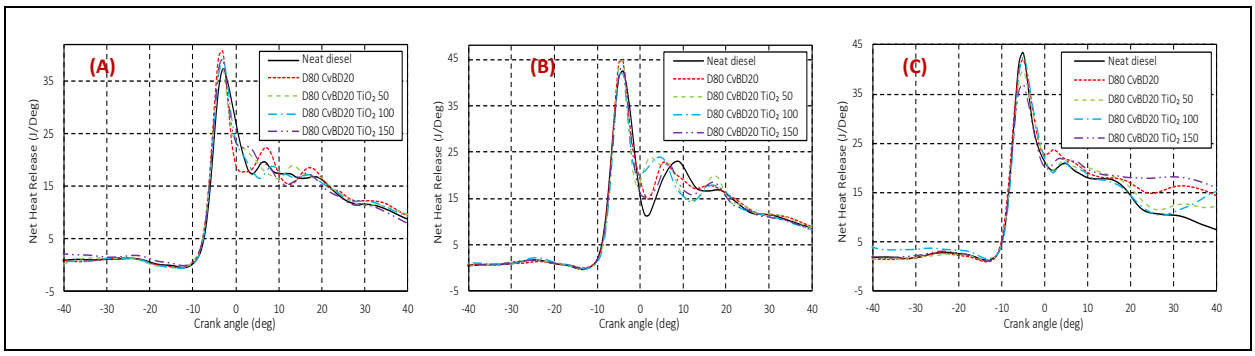


Fig. 10: Variation in net heat release at (A) 17, (B) 17.5 and (C) 18 CR

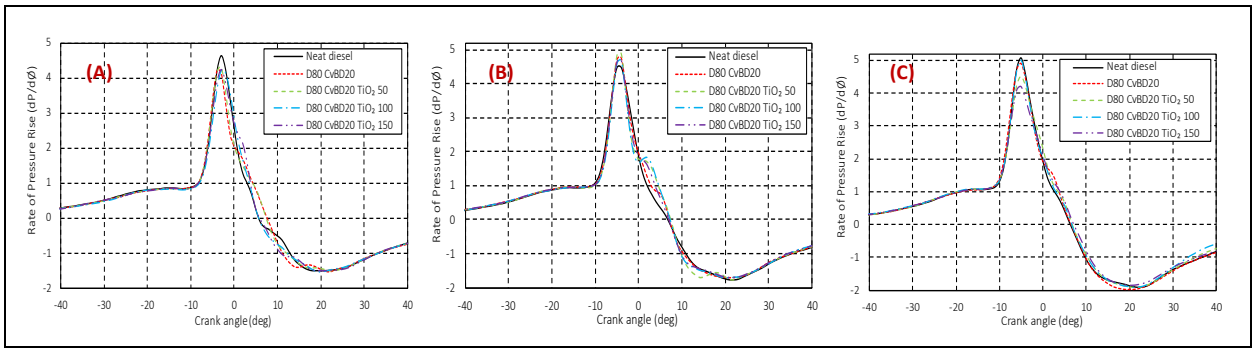


Fig. 11: Variation in rate of pressure rise at (A) 17, (B) 17.5 and (C) 18 CR

The BSFC values for 17 compression ratio (CR) blends were recorded as 0.2472, 0.3727, 0.264, 0.255, and 0.265 kg/kW-hr, respectively, at peak load. It was observed that the D80CvBD20TiO_2 blend consumed more fuel than the other blends, likely due to its higher viscosity and density, leading to suboptimal blending of fuel and air in the cylinder (Gavhane *et al.* 2020). At a compression ratio of 17.5 under the same high load, the BSFC values for the blends D100, D80CvBD20, D80CvBD20$TiO_2$50, D80CvBD20$TiO_2$100, and D80CvBD20$TiO_2$150 were 0.24, 0.25, 0.24, 0.25, and 0.27 kg/kW-hr, respectively. Among the nanoparticle-enhanced blends, D80CvBD20$TiO_2$150 exhibited the lowest BSFC, possibly due to enriched combustion enabled by the TiO_2 additive. The additive likely enhanced the blend's miscibility, resulting in reduced fuel consumption and enhanced combustion. At the highest load and a compression ratio of 18, the BSFC for the same blends was witnessed as 0.27, 0.31, 0.27, 0.28, and 0.27 kg/kW-hr. Comparing the blends, D80CvBD20$TiO_2$150 demonstrated the lowest fuel consumption, closely resembling that of pure diesel fuel.

4.1.2 Brake Thermal Efficiency (BTE)

The brake thermal efficiency of an engine is calculated by the relationship of brake power to fuel power. Fig. 4 (A, B, C) illustrates the deviation of BMEP with BTE. At a compression ratio of 17 under full load, the thermal efficiencies of diesel and its blends were found to be 35.15% (D100), 30.89% (D80CvBD20), 30.60% (D80CvBD20$TiO_2$50), 32.62% (D80CvBD20$TiO_2$100), and 30.68% (D80CvBD20$TiO_2$150). Among the blends,

D80CvBD20$TiO_2$100 had the closest thermal efficiency to pure diesel, with the highest efficiency being recorded for this blend. This could be accredited to the increased availability of oxygen, leading to more efficient combustion. In contrast, the other biodiesel blends may have suffered from higher surface tension, which could negatively impact atomization and reduce engine performance. When the compression ratio was augmented to 17.5, the thermal efficiencies observed were 35.87% (D100), 33.22% (D80CvBD20), 31.55% (D80CvBD20$TiO_2$50), 34.34% (D80CvBD20$TiO_2$100), and 31.58% (D80CvBD20$TiO_2$150). As the compression ratio was amplified further to 18, the efficiencies were 39.5% (D100), 32.5% (D80CvBD20), 36.6% (D80CvBD20$TiO_2$50), 46.6% (D80CvBD20$TiO_2$100) and 43.7% (D80CvBD20$TiO_2$150). The overall trend shows that upsurge in the compression ratio led to elevated thermal efficiency, likely due to improved combustion, better miscibility, and optimal temperature conditions (Ganesan *et al.* 2020). Notably, D80CvBD20$TiO_2$100 consistently demonstrated the highest efficiency at all compression ratios.

4.2 Emission Characteristics

This section details about the emission characteristics of all the test fuel blends like the carbon monoxide, unburnt hydrocarbon (UBHC) emission, carbon dioxide and nitrogen oxide emission.

4.2.1 Unburnt Hydro-carbon Emission

Hydrocarbon emissions are typically caused by incomplete combustion, carbon deposits in crevice volumes, and low combustion temperatures. Fig. 5 (A, B, C) illustrates the variations in unburnt hydrocarbon UBHC emissions. At higher loads, UBHC emissions were measured at 58 ppm for D100 and 57 ppm for D80CvBD20. With the increase in concentration of titanium-oxide nano-particles, the emissions for D80CvBD20$TiO_2$50, D80CvBD20$TiO_2$100, and D80CvBD20$TiO_2$150 were 56, 48, and 50 ppm, respectively. As the compression ratio was increased to 17.5, the UBHC emissions at higher loads decreased slightly to 45 ppm for D100 and 47 ppm for D80CvBD20, while the nanoparticles-enhanced blends D80CvBD20$TiO_2$50, D80CvBD20$TiO_2$100, and D80CvBD20$TiO_2$150 emitted 55, 54, and 53 ppm, respectively. At a compression ratio of 18, the emissions for D100 and D80CvBD20 at higher loads were recorded at 50.4 ppm and 50.76 ppm, respectively, while the nanoparticles-enriched blends D80CvBD20$TiO_2$50, D80CvBD20$TiO_2$100, and D80CvBD20$TiO_2$150 exhibited UBHC emissions of 63.25 ppm and 64.8 ppm during high loads (Heidari *et al.* 2020).

4.2.2 Oxides of Nitrogen Emission

At higher temperatures within the combustion region, oxygen and nitrogen reacts with each other resulting in the development of nitrogen oxides (NO_x). Fig. 6 (A, B, C) highlights the variations in NO_x emissions. Under full load at a CR of 17, the NO_x emissions for D100, D80CvBD20, D80CvBD20$TiO_2$50, D80CvBD20$TiO_2$100, and D80CvBD20$TiO_2$150 were recorded as 1621, 1703, 1811, 1830, and 1821 ppm, respectively. The biodiesel blends usually exhibited marginally higher NO_x emissions compared to pure diesel, suggesting that the improved combustion due to reduced viscosity and biodiesel's higher oxygen content might have elevated combustion temperatures, leading to increased NO_x formation *via* the Zeldovich Mechanism (Sathish *et al*. 2023). As the compression ratio increased to 17.5, NO_x emissions for D100, D80CvBD20, D80CvBD20$TiO_2$50, D80CvBD20$TiO_2$100, and D80CvBD20$TiO_2$150 were measured at 1744, 1762, 1785, 1775, and 1690 ppm, respectively. With a further increase in the CR to 18, the NO_x emissions rose to 1953 ppm for D100, 1707 ppm for D80CvBD20, 2060 ppm for D80CvBD20$TiO_2$50, 2254 ppm for D80CvBD20$TiO_2$100, and 2204 ppm for D80CvBD20$TiO_2$150.

4.2.3 Carbon Dioxide Emission

Fig. 7 (A, B, C) illustrates the deviation of carbon-dioxide emissions in relation to BMEP for different fuel blends at all load levels and a CR of 17, including D100, D80CvBD20, D80CvBD20$TiO_2$50, D80CvBD20$TiO_2$100, and D80CvBD20$TiO_2$150. Carbon dioxide emissions increased as the load increased, with biodiesel blends showing lower CO_2 levels due to their higher oxygen content. At full load, the CO_2 emissions were recorded as 8.8%, 8.9%, 8.9%, 8.7%, and 8.4% for D100, D80CvBD20, D80CvBD20TiO_2 50, D80CvBD20$TiO_2$100, and D80CvBD20$TiO_2$150, respectively. The higher oxygen availability in biodiesel blends facilitates the formation of CO_2 from carbon monoxide which is considered more environmentally acceptable since CO_2 at ground levels is more manageable compared to the toxic effects of CO emissions (Fangsuwannarak *et al.* 2013). At a CR of 17.5, the CO_2 emissions for the same fuel blends were 8.85%, 9.17%, 8.93%, 8.54%, and 8.68%, respectively. Similarly, for a CR of 18, the CO_2 percentages recorded were 9.12%, 9.23%, 9.18%, 8.37%, and 8.42% for D100, D80CvBD20, D80CvBD20$TiO_2$50, D80CvBD20$TiO_2$100, and D80CvBD20$TiO_2$150, respectively.

4.2.4 CO Emission

Partial combustion within cylinder of the engine is a major cause of carbon-monoxide formation. Fig. 8 (A, B, C) highlights the CO emissions for all tested fuel blends across different compression ratios. Incorporating nanoparticles into biodiesel blends enhances engine efficacy through their catalytic effects, leading to a notable reduction in CO emissions. Many studies have consistently shown that the biodiesel infused with nanoparticles significantly lowers CO emissions

compared to both traditional diesel fuel and pure biodiesel. The findings for CO emissions at a compression ratio of 17 for D100, D80CvBD20, D80CvBD20 $TiO_2$50, D80CvBD20 $TiO_2$100, and D80CvBD20 $TiO_2$150, with values recorded at 0.12%, 0.14%, 0.28%, 0.20%, and 0.34%, respectively are presented. At a CR of 17.5, the existence of titanium oxide nano-particles in *Chlorella* biodiesel blends resulted in CO emissions of 0.11%, 0.125%, 0.25%, 0.225%, and 0.313% for D100, D80CvBD20, D80CvBD20$TiO_2$50, D80CvBD20$TiO_2$100, and D80CvBD20$TiO_2$150, respectively. Similarly, for a compression ratio of 18, the CO emission values for the same fuel blends were measured as 0.16%, 0.13%, 0.27%, 0.28%, and 0.36%. Adding TiO_2 nanoparticles to *Chlorella* biodiesel blends boosts combustion efficiency by supplying extra oxygen for the combustion reactions, which in turn reduces CO emissions. This enhanced combustion process aids in converting CO into CO_2, leading to a further decrease in CO levels (Yoon *et al*. 2011).

4.3 Combustion Characteristics

4.3.1 In-cylinder Pressure

The in-cylinder pressure profiles for various fuels, including diesel, *Chlorella* biodiesel blends, and fuels enriched with nanoparticles are depicted here. The observed increase in cylinder pressure is linked to improved combustion efficiency, which is enhanced by the catalytic effects of the nanoparticles. The combustion process is examined by analysing the relationship between in-cylinder pressure and crank angle during the compression and expansion strokes of a 4-stroke diesel engine using different fuel blends. Fig. 9 (A, B, C) shows the variations in in-cylinder pressure with crank angle at full load for *Chlorella* biodiesel blends and diesel, measured at CR of 17:1, 17.5:1, and 18:1. The steeper pressure slopes observed with *Chlorella* biodiesel blends suggest earlier combustion initiation compared to diesel, likely due to the higher cetane numbers of the biodiesel, which shorten ignition delay. During the full load condition and at the CR of 17:1, the D80CvBD20$TiO_2$100 blend exhibited the lowest peak cylinder pressure (PCP) at 55.83 bar, followed by diesel at 57 bar, D80CvBD20$TiO_2$50 at 57.47 bar, D80CvBD20 at 57.71 bar, and D80CvBD20$TiO_2$150 at 57.8 bar. With the compression ratio increased to 17.5:1, D80CvBD20 recorded the highest PCP of 64.11 bar, followed by D80CvBD20$TiO_2$100 at 63.45 bar, D80CvBD20$TiO_2$50 at 63.31 bar, D80CvBD20$TiO_2$150 at 62.78 bar, and diesel at 61.47 bar. The increased PCP in the *Chlorella* biodiesel blends compared to diesel at peak load is attributed to the higher cetane numbers and increased oxygen content, which shorten ignition delay and enhance combustion efficiency (Chisti *et al.* 2007). At a CR of 18:1, the PCP rose for all fuels tested under full load, the PCPs for D100, D80CvBD20, D80CvBD20$TiO_2$50, D80CvBD20$TiO_2$100, and D80CvBD20$TiO_2$150 were recorded as 66.7 bar, 69.61 bar, 66.57 bar, 67.71 bar, and 65.75 bar, respectively. The increase in compression ratio reduces the effective cylinder volume, leading to higher gas temperatures and pressures. Higher compression ratios also improve fuel atomization and mixing, resulting in more complete combustion, which likely contributes to the observed rise in PCP for all fuel blends.

4.3.2 Net Heat Release Rate (NHRR)

The net heat release rate is a key parameter for assessing engine combustion, as it offers valuable information on the onset of combustion, the quantity of fuel burned during the premixed phase, and the overall intensity and duration of combustion. It also reveals differences in combustion rates across various fuels. Fig. 10 (A, B, C) illustrates the variations in NHRR with respect to crank angle for *Chlorella* biodiesel blends and diesel at CR of 17:1, 17.5:1, and 18:1, all under full load conditions. As the engine load rises, more fuel is consumed, resulting in an increased NHRR for all fuel blends. At the compression ratio of 17:1, the heat release for the fuel blends D100, D80CvBD20, D80CvBD20$TiO_2$50, D80CvBD20$TiO_2$100, and D80CvBD20$TiO_2$150 is recorded as 37.36, 40.61, 37.6, 39.17, and 39.16 J/^{o}CA, respectively. The lower ignition delay and early combustion associated with *Chlorella* biodiesel nanoparticles blends result in a lower NHRR during the premixed combustion phase. At a CR of 17.5:1, the NHRR for D100, D80CvBD20, D80CvBD20$TiO_2$50, D80CvBD20$TiO_2$100, and D80CvBD20$TiO_2$150 are 42.34, 44.54, 44.47, 41.75, and 43.79 J/^{o}CA, respectively. After reaching the peak HRR, a sudden decline occurs in all blends, likely due to heat losses from fuel vaporization. At a higher CR of 18:1, the NHRR for the fuel blends D100, D80CvBD20, D80CvBD20$TiO_2$50, D80CvBD20$TiO_2$100, and D80CvBD20$TiO_2$150 is recorded as 43.45, 41.88, 39.79, 42.77, and 36.96 J/^{o}CA, respectively, indicating a reduction in NHRR for all fuels. With the increase in compression from 17:1 to 18:1, the peak NHRR moved closer to top dead centre. While the premixed combustion phase was less intense for the *Chlorella* biodiesel and nanoparticle blends compared to diesel, the NHRR increased during the later combustion phase, signifying an extended combustion duration.

4.3.3 Rate of Pressure Rise (ROPR)

Fig. 11 (A, B, C) illustrates the rate of pressure rise in relation to crank angle for different fuel compositions under high load conditions. At a CR of 17:1, the pressure rise for the fuel blends D100, D80CvBD20, D80CvBD20$TiO_2$50, D80CvBD20$TiO_2$100, and D80CvBD20$TiO_2$150 is recorded as 4.62, 4.2, 4.32, 4.21, and 4.25 bar, respectively. For a CR of 17.5:1, the same blends show pressure rises of 4.49, 4.75, 4.87, 4.67, and 4.68 bar,

respectively. When the compression ratio is further increased to 18:1, the values of pressure rise rate were 5.08, 4.91, 4.51, 5, and 4.2 bar, respectively. When the blended fuel enters the combustion chamber at elevated temperatures, it undergoes secondary atomization and micro-explosion, causing immediate combustion and a swift increase in pressure (Hariram *et al.* 2021). Of all the nanoparticles fuel blends tested, D80CvBD20$TiO_2$100 exhibits the highest rate of pressure increase.

5. CONCLUSION

This study examined how the combustion, emission, and performance characteristics of various fuel blends were affected by the addition of nano-additive titanium oxide. At different compression ratios, the performance, emission and combustion phenomenon of diesel engines were investigated. The analysis for all the fuel blends detailed that D80CvBD20$TiO_2$100 fuel blend had the best fuel consumption, thermal efficiency, significant reduction of UBHC, and CO emissions and increased NO_x, and CO_2 emission. Based on the above recommendations, *Chlorella* biodiesel is identified as a promising alternative to diesel fuel, and among the nanoparticle blends, D80CvBD20$TiO_2$100 is the most effective and suitable for use as fuel.

FUNDING

This research received no specific grant from any funding agency in the public, commercial, or not-for-profit sectors.

CONFLICTS OF INTEREST

The authors declare that there is no conflict of interest.

COPYRIGHT

This article is an open-access article distributed under the terms and conditions of the Creative Commons Attribution (CC BY) license (http://creativecommons.org/licenses/by/4.0/).

REFERENCES

Chisti, Y., Biodiesel from microalgae, *Biotechnol. Adv.,* 25(3), 294-306 (2007). https://doi.org/10.1016/j.biotechadv.2007.02.001

Dey, S., Moni Reang, N., Deb, M. and Kumar Das, P., Experimental investigation on combustion-performance-emission characteristics of nanoparticles added biodiesel blends and tribological behavior of contaminated lubricant in a diesel engine, *Energy Convers. Manag.,* 244, 114508(2021). https://doi.org/10.1016/j.enconman.2021.114508

Fangsuwannarak, K. and Triratanasirichai, K., Improvements of palm biodiesel properties by using nano- TiO_2 additive, exhaust emission and engine performance, *Renewable Energy Technol., Opt. Mechatr.,* 43, 111- 118(2013).

Ganesan, S., Kumar, J. S. and Hemanandh, J. Optimisation of CI engine parameter using blends of biodiesel by the taguchi method, *Int. J. Ambient Energy.* 41(2), 205–208(2020). https://doi.org/10.1080/01430750.2018.1456968

Gavhane, R. S., Kate, A. M., Pawar, A., Soudagar, M. E. M. and Fayaz, H., Effect of soybean biodiesel and copper coated zinc oxide nanoparticles on enhancement of diesel engine characteristics, *Energy Sources Part A.,* 47(1), 3547–3565(2020). https://doi.org/10.1080/15567036.2020.1856237

Gowtham, M. and Prakash, R., Control of regulated and unregulated emissions from a CI engine using reformulated nano fuel emulsions, *Fuel.*, 271, 117596 (2020). https://doi.org/10.1016/j.fuel.2020.117596

Hariram, V., John, J. Godwin., Seralathan, S., Micha Premkumar, T. Comparative analysis of combustion, performance and emission phenomenon of a CI engine fuelled with algal and cotton seed biodiesel, *Int. J. Ambient Energy*, 42(6), 636 – 647 (2021). https://doi.org/10.1080/01430750.2018.1562977

Heidari, M. A., Gundoshmian, T, M., Karimi, B., Jahanbakhshi, A. and Ghobadian, B., A novel fuel based on biocompatible nanoparticles and ethanolbiodiesel blends to improve diesel engines performance and reduce exhaust emissions, *Fuel*., 276, 118079(2020). https://doi.org/10.1016/j.fuel.2020.118079

Janakiraman, S., Lakshmanan, T., Chandran, V. and Subramani, L., Comparative behavior of various nano additives in a diesel engine powered by novel Garcinia gummi-gutta biodiesel, *J. Cleaner Prod.,* 245, 118940(2020). https://doi.org/10.1016/j.jclepro.2019.118940

John, G., Hariram, V. and Seralathan, S., Emission reduction using improved fuel properties of algal oil biodiesel and its blends, *Energy Sources Part A.,* 40(1), 45-53(2018). https://doi.org/10.1080/15567036.2017.1405108

Karthikeyan, S., Elango, A., Prathima, A. and Raja, K., Environmental effects of nano additive Co3O4 in grape seed oil biofuel fuelled in CI engine, *Res. J. Chem. Environ.,* 18 (5), 14–18 (2014).

Manikandan, G., Karthikeyan, K., and Gokul, S., Experimental evaluation of A CI engine running on blends of diesel and methanol fuel with copper oxide nano particles, *Int. J. Sci. Technol. Res*., 9 (1), 247–251 (2020).

Mathimani, T., Lakshmanan U. and Dharmar P., Homogeneous acid catalysed transesterification of marine microalga *Chlorella* sp. BDUG 91771 lipid e-An efficient biodiesel yield and its characterization, *Renewable energy.,* 81, 523-533(2015). https://doi.org/10.1016/j.renene.2015.03.059

Mehregan, M. and Moghiman, M., Experimental investigation of the distinct effects of nanoparticles addition and urea-SCR after-treatment system on NO_x emissions in a blended-biodiesel fueled internal combustion engine, *Fuel*., 386, 134541(2020). https://doi.org/10.1016/j.fuel.2025.134541

Mirbagheri, S. A., Safieddin, A. S. M. and Deh, K. M. K., Modeling of the engine performance and exhaust emissions characteristics of a single-cylinder diesel using nano-biochar added into ethanol-biodiesel-diesel blends, *Fuel*., 278, 118238(2020). https://doi.org/10.1016/j.fuel.2020.118238

Sathish, T., Saravanan, R., Rajasimman, M., Ghfar, A. A. and Ramkumar, V., Nanoparticle assorted biofuels production from biowastes through transesterification, *Fuel*., 331, 125875(2023). https://doi.org/10.1016/j.fuel.2022.125875

Vellaiyan, S. and Partheeban, C. M. A., Combined effect of water emulsion and ZnO nanoparticle on emissions pattern of soybean biodiesel fuelled diesel engine, *Renew. Energy*., 149, 1157–1166(2020). https://doi.org/10.1016/j.renene.2019.10.101

Yoon, S, H. and Lee, C. S., Effect of biofuels combustion on the nanoparticle and emission characteristics of a common-rail di diesel engine, *Fuel*., 90(10), 3071–3077 (2011). https://doi.org/10.1016/j.fuel.2011.05.007